phys. stat. sol. (a) **203**, No. 1, 142–148 (2006) / **DOI** 10.1002/pssa.200563503

Characterization of crystallographic properties and defects via X-ray microdiffraction in GaN (0001) layers

R. I. Barabash[*, 1], **O. M. Barabash**[1], **G. E. Ice**[1], **C. Roder**[2], **S. Figge**[2], **S. Einfeldt**[**, 2], **D. Hommel**[2], **T. M. Katona**[3], **J. S. Speck**[4], **S. P. DenBaars**[4], and **R. F. Davis**[5]

[1] Metals and Ceramics Div., Oak Ridge National Laboratory, Oak Ridge, TN 37831, USA
[2] Institute of Solid State Physics, University of Bremen, P.O. Box 330 440, 28334 Bremen, Germany
[3] Electrical and Computer Engineering Department, College of Engineering, University of California at Santa Barbara, Santa Barbara 93106, USA
[4] Materials Department, College of Engineering, University of California at Santa Barbara, Santa Barbara 93106, USA
[5] Materials Science and Engineering Department, North Carolina State University, Raleigh, USA

Received 27 August 2005, revised 2 November 2005, accepted 2 November 2005
Published online 4 January 2006

PACS 61.10.Nz, 68.37.Hk, 68.55.Jk, 68.55.Ln, 68.60.Bs, 81.15.Gh

Intrinsic stresses due to lattice mismatch, high densities of threading dislocations, and extrinsic stresses resulting from the mismatch in the coefficients of thermal expansion, are present in almost all III-Nitride heterostructures. Stress relaxation in the GaN layers occurs in conventional, cantilever (CE) and in pendeo-epitaxial (PE) films via the formation of additional misfit dislocations, domain boundaries, elastic strain and wing tilt. Polychromatic X-ray microdiffraction, high resolution monochromatic X-ray diffraction and SEM analysis have been used to determine the crystallographic properties, misfit dislocations distribution and crystallographic tilts in uncoalesced GaN layers grown by PE and CE. The crystallographic tilt between the GaN(0001) and Si(111) planes was detected in the CE grown samples on Si(111). In contrast there was no tilt between GaN(0001) and SiC(0001) planes in PE grown samples. The wings are tilted upward for both the PE and CE grown uncoalesced GaN layers.

© 2006 WILEY-VCH Verlag GmbH & Co. KGaA, Weinheim

1 Introduction

GaN films are typically grown on sapphire or SiC substrates which results in a high density (10^8 to 10^{10} cm^{-2}) of threading dislocations [1, 2]. These dislocations impact many material properties such as the minority carrier lifetime and the mobility. The performance of light emitting devices is particularly impaired as dislocations are known to act as non-radiative recombination centers; when the dislocation density is reduced, the threshold current density of laser-diodes usually decreases and the device lifetime increases. Lateral epitaxial overgrowth techniques such as pendeo-epitaxy (PE) [3–7] and cantilever-epitaxy (CE) [8–10] have been developed to reduce a number of defects inherited from the substrate. In both techniques GaN layers grow overhanging the trenches. In this paper we compare structural properties of four samples: two of them grown by CE and two grown by PE. A combination of polychromatic X-ray microdiffraction (PXM), high resolution X-ray diffraction (HRXRD) and scanning electron microscopy (SEM) provides detailed new information about the local distortion field and misfit dislocations distribution, the misorientations between the GaN layer, the substrate and the wing tilt in GaN layers

* Contact author: e-mail: barabashr@ornl.gov
** Present address: Ferdinand-Braun-Institut, Gustav-Kirchhoff-Str. 4, 12489 Berlin, Germany

© 2006 WILEY-VCH Verlag GmbH & Co. KGaA, Weinheim

grown by CE and PE. Application of PXM allows to get direct experimental verification of the finite element simulations [3] about the wing tilt direction in PE grown samples and to compare tilts in CE and PE grown samples.

2 Experiment

In the two PE samples GaN stripes along $[1\bar{1}00]$ direction having a rectangular cross section were etched from 1 μm thick GaN layers grown by metalorganic vapor phase epitaxy on 0.1 μm thick AlN buffer layers previously deposited on 6H-SiC (0001) substrates. The subsequent overgrowth process was stopped before the wings coalesced into a layer. Further details of the PE growth process can be found in Refs. [3, 9]. The two PE grown samples differed in their GaN stripe geometries: The GaN thickness, the column width and the wing width were 1.46 μm, 3.80 μm, and 0.98 μm for PE-B sample and 3.53 μm, 3.46 μm and 1.74 μm for PE-A sample.

CE samples were grown on Si(111) substrates. They consist of 5 μm wide Si mesas separated by 5 μm wide trenches along the $\mathrm{Si}[11\bar{2}]$ direction. The etch depth is approximately 5 μm. The substrate was overgrown with a 100 nm thick AlN nucleation layer followed by a thick GaN layer using metal–organic vapor phase epitaxy. The growth was stopped before the coalescence of the GaN wings resulting in separate GaN stripes in the $\mathrm{GaN}[1\bar{1}00]$ direction. The two samples identical to those described in the Ref. [10] differ in their wing tilt as they were grown under different lateral/vertical growth rates: CE-A sample with higher, and CE-B sample with smaller lateral/vertical initial growth rates.

PXM was performed with a focused polychromatic synchrotron beam which hit the sample surface in an area of 0.5 μm in diameter at 45° incidence. The Laue diffraction patterns from both the GaN layer and the Si or SiC substrate were recorded with a charge-coupled device (CCD) area detector placed at 90° relative to the incident beam [11]. The Cartesian reference frame is set such that the y-axis coincides with the $[1\bar{1}00]$ direction of the GaN stripe. The x-axis is perpendicular to the stripe in the plane of the GaN film and is running in the $\mathrm{GaN}[11\bar{2}0]$ direction.

High resolution X-ray diffraction (HRXRD) measurements were performed using a Philips X'Pert MRD diffractometer equipped with a fourfold Ge(220) or a twofold hybrid monochromator in Ge(220) configuration and a threefold Ge(220) analyzer.

SEM images were collected using Philips XL30 field-emission scanning electron microscope equipped with a DigiView camera.

3 Results and discussion

The local structural quality of the GaN layers was analyzed by PXM. The small PXM microbeam (~0.5 μm) makes it possible to characterize the local structural information from different regions of the stripe. In contrast HRXRD (size of the beam 0.5 mm) gives the information averaged over ~50 stripes. PXM is well suited for the analysis of the deviatoric strain fields and local distribution of Geometrically Necessary (unpaired) Dislocations (GNDs) as well as misfit dislocations (MD) and Geometrically Necessary Boundaries (GNBs) at the micron and submicron levels [11]. To obtain statistically reliable information about the different regions of the GaN column and wings and the Si or SiC substrate the sample was scanned under the white microbeam. For these line scans Laue patterns were collected at 1000 different points with 0.5 μm spacing along the line. Approximately 10–20 parallel line scans with the step size of 1 μm were recorded to obtain a two-dimensional (2D) map of the sample. The 2D map presented in Fig. 1 for a PE grown sample shows the $(\bar{1}08)$ GaN Laue spot (in the center of each image) and two SiC reflections below and above it. Images obtained from the column region, left and right wings are indicated with dashed lines. The SiC reflections do not change position with sample translation. The SiC Laue reflections were used as a reference to determine the position of the $\mathrm{GaN}(\bar{1}08)$ Laue reflection. When the probing spot is moved along the positive x-axis and first hits the left wing, the GaN reflection appears at the right side of the SiC reflections (left wing region). When the probe is in the center of the column, the GaN reflections are aligned with the SiC reflections for both samples. With further dis-

 © 2006 WILEY-VCH Verlag GmbH & Co. KGaA, Weinheim

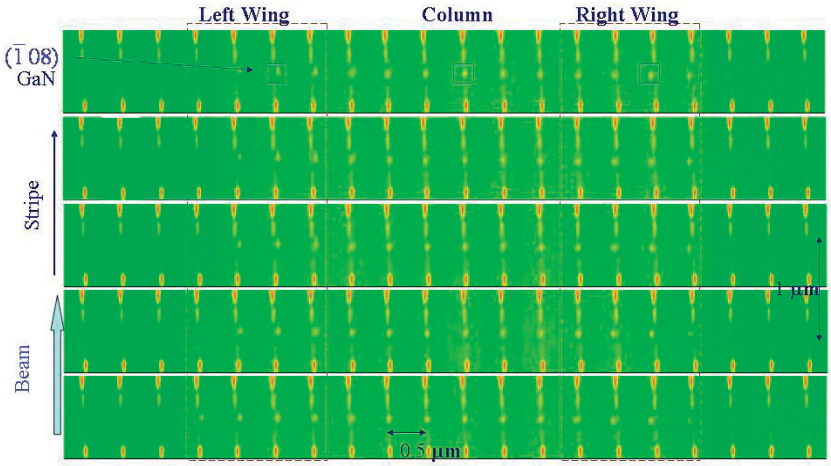

Fig. 1 Two dimensional map over the PE grown GaN layer on SiC(0001) substrate (sample PE-B). The distance between the probing locations across the stripe direction was 0.5 µm, and the distance between parallel line scans was 1 µm.

placement towards the right wing the GaN reflections appear to the left of the SiC reflections. The GaN spot disappears in the gap between the wings. The shift of the GaN reflections along with the geometry of the structure, demonstrates an upward wing tilt (relative to the column) in the PE grown samples [9]. In the same manner it was determined that in the CE grown samples the wing tilt is also upward. Similarity of the GaN Laue spot behavior in different line scans shows that the GaN layers are relatively homogeneous along the stripes. The strain, stress and wing tilt across the stripe in PE grown samples increased with the width-to-height ratio. For small width-to-height ratios (PE-A sample) the tilt is small, and it changes gradually in the region of the column. For larger width-to-height ratios the tilt is higher, and it changes abruptly at the wing/column interface. PXM analysis of the wing tilt in CE grown samples shows that it is ~0.6° for CE-A and ~0.036° for CE-B samples. In the PE grown samples the wing tilt was 0.159° and 0.085° for PE-B and PE-A samples. The findings of PXM are in good agreement with the results of HRXRD measurements for all measured samples. Interestingly the CE-A sample has a higher wing tilt than in PE samples, and the CE-B sample has a lower wing tilt than the PE samples. Thus the scatter of the wing tilt values is higher for CE grown samples than for the PE grown ones.

With a polychromatic X-ray spectrum Ewalds construction of the measurable reflections in reciprocal space is performed with Ewald spheres with a range of radii. The micro-Laue is sensitive to radial line integrals through reciprocal space. For example GaN reflections of the (000*h*) type are superimposed in the Laue pattern. Similarly the Si(111) reflection in CE grown samples or SiC(0001) in PE grown samples can also be superimposed to the GaN(000*h*) reflections if the GaN(0001) plane is parallel to the Si(111) or SiC(0001) plane (Fig. 2a). The Laue patterns in Fig. 2b (CE-A and CE-B) demonstrate that the GaN(0006) and the Si(444) reflections are displaced relative to each other along the *y*-axis but coincide at the center of the stripe along the *x*-axis. This indicates that the GaN(0001) and the Si(111) planes are not parallel to each other; there is a tilt between these two in the direction parallel to the stripes. For sample CE-A and CE-B this tilt amounts to ~1.5° and ~0.5°, respectively. HRXRD measurements reveal tilt values of 1.6° and 0.68°, respectively. In the contrast, the PE grown GaN on SiC(0001) substrates demonstrates good alignment between GaN(0001)and SiC(0001) surface planes in the direction parallel to stripes (Fig. 2 bottom). We note that the two different kinds of tilts are demonstrated in the data: wing tilt manifests itself by the horizontal displacement of the Laue diffraction between substrate and GaN spots in the Laue patterns at the wing regions (Fig. 1), while the crystallographic tilt between the GaN(0001) and Si(111) planes for CE grown samples, is observed by the vertical separation of the spots for CE samples (absent, for example, in the data of the sample grown by PE).

© 2006 WILEY-VCH Verlag GmbH & Co. KGaA, Weinheim

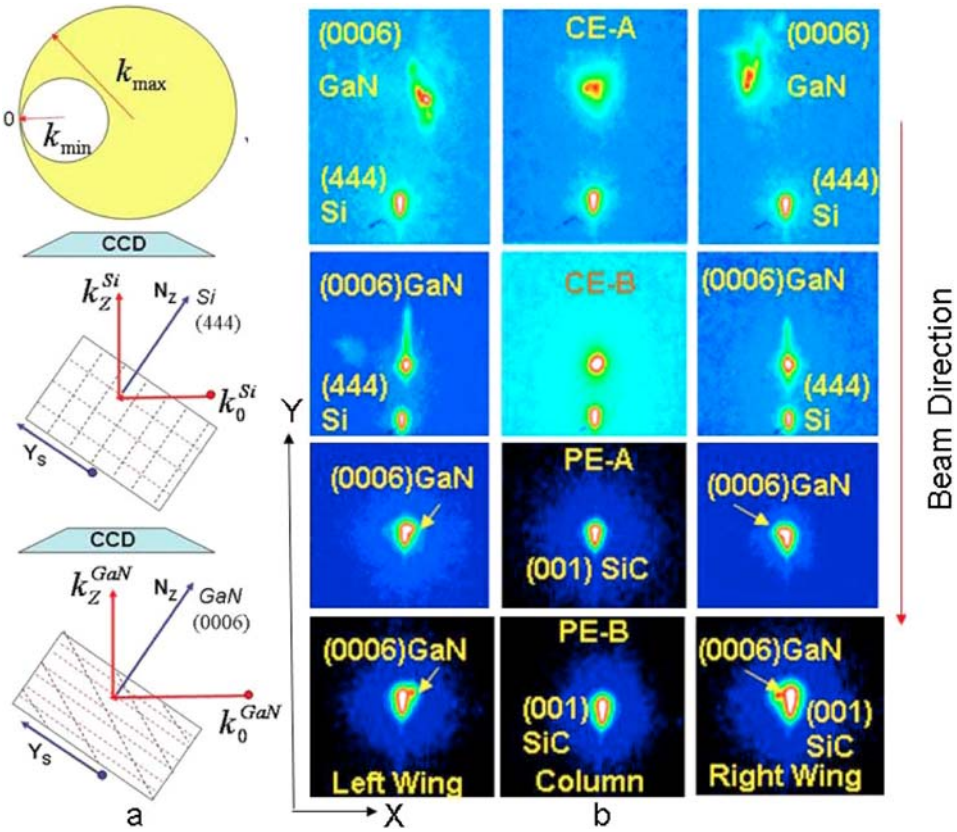

Fig. 2 (a) Sketch of the white beam geometry demonstrating that parallel planes of the GaN and substrate are projected at the same position on the CCD; (b) central region of the Laue pattern for CE-A and CE-B samples (top) and for PE-A and PE-B grown samples (bottom). Vertical displacement between the GaN(0006) and Si(444) Laue spots is due to crystallographic tilt between GaN(0001) and Si(111) planes. Such tilt is not observed for PE samples.

In PXM analysis straight edge dislocations with lines parallel to the diffraction vector do not influence the scattering intensity (as opposed to screw dislocations) [11]. For this reason the specular (0006)GaN Laue spot is not sensitive to the edge threading dislocations (similar to HRXRD) but it is sensitive to the screw portion of threading dislocations. In contrast, misfit dislocations (MDs) cause a cumulative local lattice curvature in the GaN layer, which is conveniently measured with PXM. The Laue spot obtained from the curved region is elongated (streaked) in a certain, ξ, direction. The streak direction depends both on the orientation and the number of MDs (their Burgers vector, $\boldsymbol{b}$, and line direction, τ) in the probed volume and on the orientation of the measured Laue spot, $\boldsymbol{G}_{hkl}$. The full width at half maximum in the streak direction, FWHM_ξ, scales linearly with the density of MDs, n^{MD}, and with the size of the probed GaN layer, L [11]:

$$\mathrm{FWHM}_\xi \propto n^{\mathrm{MD}} L f_\xi(\hat{\tau}\hat{G}_{hkl}) \ , \tag{1}$$

where $f_\xi(\hat{\tau}\hat{G}_{hkl})$ is the so called contrast factor along the streak depending on the angle between the dislocation line, τ and the diffraction vector directions, $\boldsymbol{G}_{hkl}$. Groupings of dislocations within a dislocation wall causes inhomogeneous lattice curvature in the near wall region, and the Laue spot splits into several spikes [11].

 © 2006 WILEY-VCH Verlag GmbH & Co. KGaA, Weinheim

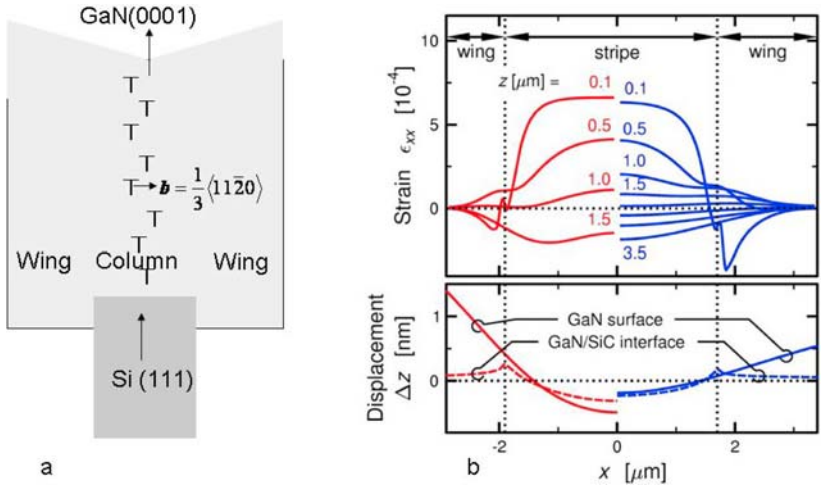

Fig. 3 Scheme showing formation of MD(1) dislocations in the column region (a) and FE simulations results of strain and displacements distribution for PE-A (blue) and PE-B (red) samples.

The intensity distribution of the (0006)GaN Laue spot in the column region of the CE-A sample typically consists of two pronounced spikes in the directions perpendicular to the stripe indicating the formation of a tilt dislocation array. PXM method allows for the characterization of the dislocation distribution within such an array. The local tilt angle in the middle of the overgrown region near the center of the column is always much smaller then the total tilt between wings. We measure a tilt angle at the center of the column of $\vartheta = \vartheta_1 \approx 0.12°$ for the CE-A sample and assuming pure edge MD(1) dislocations with Burgers vector perpendicular to the stripes $b = \frac{1}{3}\langle 11\bar{2}0\rangle$ and dislocation lines running parallel to the stripe directions we obtain the distance between these dislocations in the tilt boundary $h_A = 50c$ (Fig. 3). Here c is the interatomic distance along the z-axis of the GaN. These dislocations are similar to the type B dislocations observed by Lilliental-Weber et al. [12] and to D1 type defects observed by Sakai et al. [5]. For a GaN column with the thickness of ~4.4 μm in the CE-A sample this amounts to 168 dislocations in the tilt dislocation array. Not all dislocations are grouped within the boundary. Some dislocations remain randomly distributed. The total density of the above MDs in the column region of the CE-A sample is equal to $n^{MD} \approx 3.8 \times 10^9$ cm^{-2}. This results in the deviatoric component of the distortion tensor $\omega_{XZ} = -\omega_{ZX} = 0.004$ in the CE-A column region. This distortion field is antisymmetric and represents a local rotation about the y-axis in the CE-A column region. In contrast spiking of the (0001)GaN spot was not observed in the CE-B sample (with the smallest wing tilt), thus indicating that dislocation arrays did not form in that sample. The ω_{XZ} component of the distortion tensor for CE-B sample in the column region (derived from the Laue spot intensity distribution along the X-direction) is equal: $\omega_{XZ} = -\omega_{ZX} = 0.0013$. For full relaxation it would take $n^{MD} \approx 1.5 \times 10^9$ cm^{-2} density of misfit dislocations. However the analysis of the intensity profile of the CE-B sample in X-direction suggests that there was no essential relaxation in that sample.

Similar tilt boundaries were observed in the PE-B sample at the column/wing interface with misfit dislocations (1). The distances between MD(1) type dislocations in the tilt interface boundary was found to be $h_{PE\text{-}B} = 98c$ for PE-B and $h_{PE\text{-}A} = 294c$ for PE-A samples.

The MD(1) type dislocations cause maximal streaking of the (0006)GaN Laue spot in X-direction however they do not contribute to the broadening of the (0006)GaN Laue spot in Y-direction (their contrast factor $f_\xi(\hat{\tau}\hat{G}_{hkl}) = 0$ along the Y-direction [11]. The elongation of the (0006)GaN Laue spot in the Y-direction was also observed in the column region. The $\omega_{YZ} = -\omega_{ZY}$ component of the distortion tensor was calculated from this broadening along the Y-direction; $\omega_{YZ} = -\omega_{ZY} = 0.0037$ and $\omega_{YZ} = -\omega_{ZY} = 0.0019$ for CE-A and for CE-B samples correspondingly. The $\omega_{YZ} = -\omega_{ZY}$ component of the distortion

© 2006 WILEY-VCH Verlag GmbH & Co. KGaA, Weinheim

field describes the local rotation in the column around the *x*-axis caused by the crystallographic tilt between the GaN(0001) and Si(111) planes. For PE-A and PE-B samples this component of the distortion tensor was equal to zero.

In the wing region of both PE and CE samples the broadening is much smaller in *X*-direction due to a reduction in the threading dislocation density. However in the wing region of the CE-A sample, the spike-like nature of the spot is observable in an almost orthogonal direction: Laue spots become elongated ~ about 30° off the stripe direction (Fig. 2b top). This indicates the formation of an MD(2) dislocation array providing tilt equal to 0.23° inclined approximately 30° to the stripe direction. These MD(2) type dislocations are formed as a result of stress relaxation in the CE-A wings caused by the deviatoric component of the distortion field equal to $\omega_{YZ} = -\omega_{ZY} = 0.0041$. According to the streak orientation, the MD(2) dislocations group mainly from edge misfit dislocations with $b = \langle 1\bar{2}10 \rangle/3$ or $b = \langle \bar{2}110 \rangle/3$ and are inclined by 30° to the stripe direction similar to the type A dislocations observed with TEM by Lilliental-Weber et al. [12]. Relaxation in this direction is not observed either in the CE-B sample or in the PE samples. For PE samples the deviatoric distortion field components $\omega_{YZ} = -\omega_{ZY} = 0$, therefore it is possible to use 2D Finite Element simulations taking into account the mismatch in thermal expansion coefficients between the GaN and the substrate (similar to the Ref. [3] for the geometry of PE-A and PE-B samples). The simulated distribution of displacements and stress/strain fields in the PE geometry are similar to experimentally observed upward wing tilts in the PE-A and PE-B samples (Fig. 3). However it is not possible to apply a similar simulations for CE grown samples. The existence of a nonzero ω_{YZ} deviatoric component of the distortion field for the CE grown samples indicates that a 3D description is necessary. The development of a more general model taking into account the 3D strain/stress distribution in CE grown samples is now underway.

The complementary plan-view SEM analysis of CE samples surface was performed (Fig. 4). Many defects and tilt boundaries were observed by SEM in the column region of the CE-A. The number of defects is reduced in the wing region of the sample A. Sharp crack-like boundaries in the CE-A sample cross both column and wings regions. Average distance between such boundaries is about 50 μm. Within these regions some smaller boundaries across the wing regions are observed with an average distance of several microns. In contrast no boundaries were observed in sample B (Fig. 4b). With SEM we obtain information about the boundary distribution at a larger scale than with PXM.

The average distance between the boundaries observed by SEM in the CE-A sample is larger than a few microns; PXM allows measurement within 0.5 μm of boundaries. The different scales of distances between the boundaries observed by SEM and PXM indicates the formation of the hierarchical dislocation structure due to the following relaxation processes in the CE-A sample: (I) at the large scale, big domains are separated by sharp crack-like boundaries passing perpendicular to the whole GaN stripe with an average distance of 50 μm; (II) at the second length scale, some smaller angle (4–5°) irregular

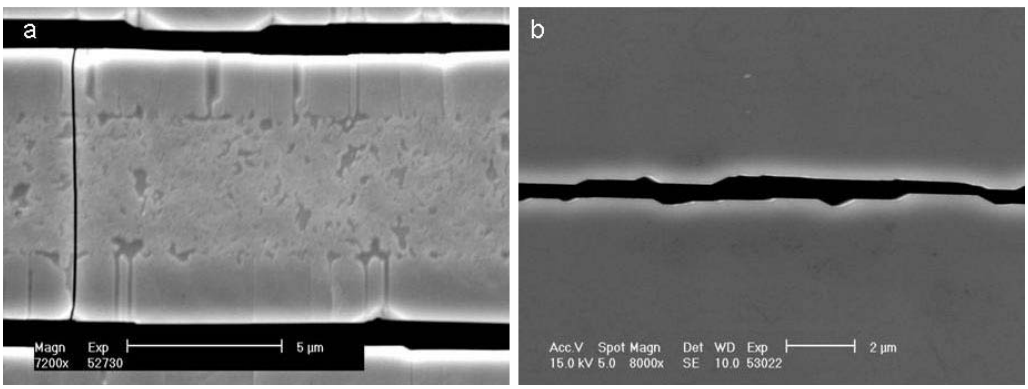

Fig. 4 SEM analysis of the surface of CE grown sample A (a) and sample B (b) samples.

 © 2006 WILEY-VCH Verlag GmbH & Co. KGaA, Weinheim

boundaries are separated by a distance of several microns; (III) at the third length scale the separate misfit dislocations and their groupings within small angle (~0.2–0.3°) dislocation walls are causing local curvature of the GaN lattice.

4 Summary

PXM results give direct experimental confirmation that the crystallographic tilt of GaN wings in GaN layers grown by CE on Si(111) or by PE on SiC(0001) substrates is upward. The threading dislocation density was reduced in the wings compared to in the columns. In CE grown samples the (001) out-of-plane GaN surface normal is crystallographically tilted relative to the Si(111) substrate. In PE grown samples the (001) surface normal of GaN and SiC are aligned parallel to each other. Misfit dislocations are formed as a result of stress relaxation in CE-A sample. This relaxation processes is suppressed in the CE-B samples. The predominant types of misfit dislocations were characterized. In the PE samples the stress/strain distribution is two dimensional, while in CE samples a three dimensional stress/strain distribution is formed.

Acknowledgement Research sponsored in part by the Division of Materials Sciences and Engineering, Office of Basic Energy Sciences and ORNL SHARE User Facility, U.S. Department of Energy, under Contract DE-AC05-00OR22725 with UT-Battelle, LLC. Data collection with PXM has been carried out on beamline ID-34-E at the Advanced Photon Source, Argonne IL. The UNICAT facility at the Advanced Photon Source (APS) is supported by the U.S. DOE under Award No. DEFG02-91ER45439, through the Frederick Seitz Materials Research Laboratory at the University of Illinois at Urbana-Champaign and the Oak Ridge National Laboratory (U.S. DOE contract DE-AC05-00OR22725 with UT-Battelle LLC. The APS is supported by the U.S. DOE, Basic Energy Sciences, Office of Science under contract No. W-31-109-ENG-38.

References

[1] S. D. Lester, F. A. Ponce, M. G. Craford, and D. A. Steigerwald, Appl. Phys. Lett. **66**, 1249 (1995).
[2] T. Metzger, R. Hopler, and E. Born, Philos. Mag. A **77**, 1013 (1998).
[3] S. Einfeldt, A. M. Roskowski, E. A. Preble, and R. F. Davis, Appl. Phys. Lett. **80**, 953 (2002).
[4] K. Linthicum, T. Gehrke, D. Thomson, E. Carlson, P. Rajagopal, T. Smith, D. Batchelor, and R. F. Davis, Appl. Phys. Lett. **75**, 196 (1999).
[5] A. Sakai, H. Sunakawa, and A. Usui, Appl. Phys. Lett. **73**, 481 (1998).
[6] R. F. Davis, S. Einfeldt, E. A. Preble, A. M. Roskowski, Z. J. Reitmeier, and P. Q. Miraglia, Acta Mater. **51**, 5961 (2003).
[7] R. Barabash, G. Ice, W. Liu, S. Einfeldt, A. M. Roskovsky, and R. F. Davis, J. Appl. Phys. **97**, 21 (2005).
[8] T. M. Katona, M. D. Craven, P. T. Fini, J. S. Speck, and S. P. DenBaars, Appl. Phys. Lett. **79**, 2907 (2001).
[9] T. M. Katona, J. S. Speck, and S. P. DenBaars, Appl. Phys. Lett. **81**, 3558 (2002).
[10] C. Roder, H. Heinke, D. Hommel, T. M. Katona, J. S. Speck, and S. P. DenBaars, J. Phys. D, Appl. Phys. A **36**, 188 (2003).
[11] R. Barabash and G. Ice, Microdiffraction Analysis of Hierarchical Dislocation Organization, in: Encyclopedia of Materials: Science and Technology Updates (Elsevier, Oxford, 2005), pp. 1–18.
[12] Z. Lilliental-Weber and D. Cherns, J. Appl. Phys. **89**(12), 7833 (2001).

© 2006 WILEY-VCH Verlag GmbH & Co. KGaA, Weinheim